International Journal of Microscopy

Yu et al., Int J Microsc 2017, 1:1

Research Article OMICS International

Mechanistic Insights of the Infiltrated Cells in Large Porous Scaffolds Based on Microscopic Analysis of the Cells in Novel Scale-Down Culture Systems

Ling Yu[1], Cai MSc[1], GuoXia Han[1] and Tao Sun[2*]

[1]*Department of Biological Sciences, Xi'an Jiaotong-Liverpool University, Suzhou, China*
[2]*Department of Chemical Engineering, Centre for Biological Engineering, Loughborough University, UK*

Abstract

Objective: Investigation of the cells cultivated within large porous scaffolds is problematic. This study aimed to develop scale-down culture models (SDCMs) for high throughput microscopic analysis of the infiltrated cells.

Methods: Due to the advantages of biocompatibility and transparency, commercial glass capillaries with different lengths (5-80 mm) and inside diameters (0.3, 1.0, 1.5, 1.7, 2.0 mm) were tailored and situated in petri-dishes to mimic the interconnected pore structures within thick porous scaffolds. For the ease of *in situ* cell assessment, both horizontal and vertical SDCMs were developed and integrated with conventional microscopic technologies.

Results: Evaluation experiments using migratory human dermal fibroblasts indicated that these SDCMs were able to simulate varying microenvironments surrounding infiltrated cells within large scaffolds. As both individual and aggregated cells at different parts of the capillaries were imaged noninvasively with sufficient high resolutions, it was feasible to track the dynamic tissue formation processes without sacrificing the delicate samples.

Conclusion: This research demonstrated that these SDCMs could rapidly provide reliable data for the mechanistic understanding of various overarching factors that contribute the colonization of the infiltrated cells in large porous scaffolds.

Keywords: Porous scaffold; Infiltrated cell; Scale-down design; Glass capillary; Tissue culture; *In situ* assessment; Fibroblast

Introduction

Tissue Engineering (TE) aims to apply the principles of engineering and life sciences toward the manufacturing of bio-substitutes for clinical or diagnostic applications [1,2]. Even though dramatic advances and developments have been made in this research field, it is still a challenge task to manufacture fully functional tissues due to several translational challenges [3,4]. First of all, the mechanistic understanding of the relationships between molecules, cells, tissues and organs as a whole during tissue regeneration is somewhat limited [2,5]. Secondly, due to the lack of sufficient understanding, diverse three-dimensional (3D) scaffolds, media and tissue culturing protocols have been developed; while there is no gold standard or generic procedure for tissue culture [3,5]. Thirdly, significant scale-up challenges still exist in TE, and new scale-up strategies based on thorough investigation of the infiltrated cells within the heterogeneous and anisotropic 3D scaffolds are urgently needed [6]. Thorough investigation of the aforementioned relationships during tissue formation based on current cell and tissue culture technologies is problematic. As the time- honoured two-dimensional (2D) cell cultures are far removed from the complexities cells encounter in real-life tissues, they are usually considered as a poor proxy of cells *in vivo* [7,8]. Tissue culture models thus have been developed to enhance the physiological relevance of experiments *in vitro* as they can provide more suitable 3D microenvironments for the cultured cells [6-9]. However, these tissue models are usually more labour intensive than 2D cell cultures [9], and it is difficult to distinguish the regulatory functions of different architectural, biochemical and biomechanical properties in the 3D culture environments [10-12]. Very recently, we developed a 3D cell culture and imaging system (3D CCIS) to investigate the action mechanism of specific structural and biochemical features [13]. Due to the utilization of very thin substrates, this 3D CCIS was not suitable for the investigation of the over-arching and dimensional factors such as the nutrient and oxygen gradients induced by large 3D scaffolds. To bridge the gap between the traditional 2D and 3D culture technologies, and also complement with the 3D CCIS, the aim of this study was to develop a set of scale-down culture models (SDCMs) for high throughput cell culture and investigation of action mechanisms of over-arching and dimensional factors on the infiltrated cells.

Due to the obvious advantages such as biocompatibility [14] and transparency, commercially available medical glass capillaries with different lengths (5-80 mm) and inside diameters (0.3, 1.0, 1.5, 1.7 and 2.0 mm) were tailored, situated in petri-dishes to mimic the interconnected pore structures within porous scaffolds. For the ease of *in situ* microscopic analysis of the infiltrated cells from different perspectives, horizontal and vertical SDCMs were fabricated and integrated with conventional microscopic technologies. The migratory human dermal fibroblast (HDF) was selected as the exemplary cell to evaluate these models, which were then utilised to systemically investigate the influences of various parameters including the thickness of scaffold on the behaviours of the cultivated cells. It was demonstrated that all these SDCMs could be used to obtain the mechanistic insights of cell infiltration and survival in large porous scaffolds, which is still an unsolved problem in Tissue Engineering [15-17].

***Corresponding author:** Tao Sun, Department of Chemical Engineering, Centre for Biological Engineering, Loughborough University, UK, Tel: +44 (0)1509 223214; E-mail: T.Sun@lboro.ac.uk

Received September 04, 2017; **Accepted** September 12, 2017; **Published** September 20, 2017

Citation: Yu L, Cai MSc, Han G, Sun T (2017) Mechanistic Insights of the Infiltrated Cells in Large Porous Scaffolds Based on Microscopic Analysis of the Cells in Novel Scale-Down Culture Systems. Int J Microsc 1: 101.

Materials and Methods

Cell culture

The methodologies for media preparation, cell isolation and culture were as described previously [18]. Briefly, HDFs were cultured in flasks with Dulbecco's modified Eagle's medium (DMEM, Sigma) supplemented with 10% (v/v) new born calf serum (NBCS, GIBCO), 2×10^{-3} mol l^{-1} glutamine (Sigma), 100I U ml^{-1} penicillin and 100 μg ml^{-1} streptomycin (Sigma), monitored using a phase contrast microscope (Nikon TS100, Japan), and detached for experiments when approximately 90% confluent.

Fabrication of the scale-down culture models (SDCMs)

Commercially available medical glass capillaries with inside diameters (IDs) from 0.3, 1.0, 1.5, 1.7 to 2.0 mm were used to fabricate three types of SDCMs. In the horizontal SDCM (Figure 1a), glass capillaries with different lengths (from 5 to 80 mm) were used to simulate the interconnected pore structures in thick porous scaffolds. Both ends of each glass capillary (1) were inserted into the small holes (same size as the capillary outside diameter) created in the centers of two square silicone chips (4 mm × 4 mm, 0.5 mm thick) (2), so the capillary was suspended horizontally in a plastic petri-dish (3). Cell suspension (2×10^5 cells ml^{-1}) (4) was added gently into the capillary and incubated at 37°C and 5% CO_2 for 2 hours for cell attachment; fresh media (5) were then added into the petri-dish to submerge the capillary for subsequent cell culture. To understand the influences of oxygen gradients in thick scaffolds on infiltrated cells, a horizontal SDCM with connected capillaries (Figure 1b) was designed. Short capillaries (5-10 mm) (1) were connected into longer ones using oxygen permeable silicone tubes (2), then suspended horizontally using 2 pieces of square silicone chips (4 mm × 4 mm, 0.5 mm thick) (3) in a petri-dish (4). Cell suspension (2×10^5 cells ml^{-1}) (5) was added into the connected capillary and incubated for 2 hours for cell attachment; fresh media (6) were then added into the petri-dish for cell culture. During cell culture using these two horizontal SDCMs, cells in border area (B, 1 mm long), near border area (NB, 1 mm long, and 5 mm away from the near border) and central area (C, 1 mm long) of the capillaries were monitored non-invasively and continuously using optical microscopes. After cell culture, the connected short capillaries were disconnected and the cells inside each of them were also analyzed separately. In order to assess the cultured cells from a different perspective, a vertical SDCM (Figure 1c) was fabricated. A short capillary (10 to 15 mm in length) (1) was vertically inserted into the small hole created in a (2) horizontally orientated supporting silicone sheet with 3 short glass rods (3) attached underneath as the legs. For cell seeding, the supporting silicone sheet was first rotated to keep the short capillary horizontal, cell suspension (2×10^5 cells ml^{-1}) (4) was added gently into the capillary and incubated for cell attachment. The short capillary was then re-orientated vertically and situated in a petri-dish (5), and fresh media (6) were added into the dish to submerge the lower part of the capillary with seeded cells for further cell culture. During cell culture, the cells in the lower part of the capillary (1mm long) were monitored non-invasively and continuously. *In situ* analysis of the cells inside all these three SDCMs was carried out by simply putting the petri-dishes on the stages of inverted phase contrast microscope (Nikon TS100, Japan) or live-cell fluorescent microscope (Nikon Ti, Japan) and imaging the cells from underneath the petri-dishes. In this research, multiple capillaries with different IDs and lengths were fabricated and situated in plastic petri-dishes (9 cm in diameter) to parallelize cell culture experiments. Before cell seeding, all the capillaries were sterilized with 70% ethanol for 24 h, washed thoroughly with phosphate buffered saline (PBS×3), sterile distilled water (×3) and dried.

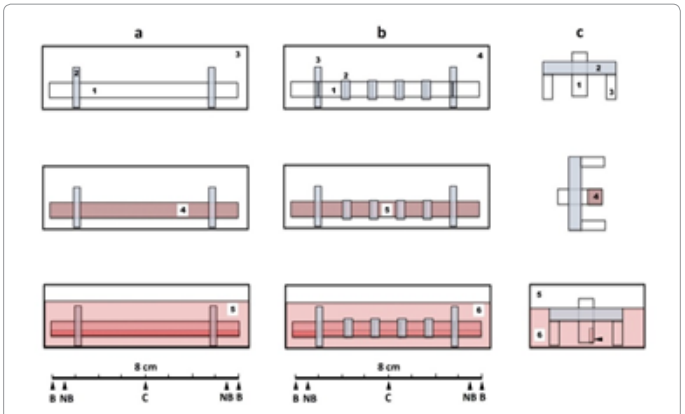

Figure 1: **(a)** Schematic diagram of the cross sections of the horizontal scale-down culture model (SDCM) with a long glass capillary (80 mm). The (1) capillary was suspended horizontally by inserting each end into a small hole (same outside diameter as the capillary) created in the center of a (2) square silicone chip (4 mm × 4 mm, 0.5 mm thick). The horizontal capillary was then situated in a (3) plastic petri-dish. After system sterilization, (4) cell suspension (2×10^5 cells ml^{-1} in DMEM) was added gently into the capillary and incubated at 37°C and 5% CO_2 for 2 hours for cell attachment, (5) media were then added into the petri-dish to submerge the capillary for cell culture. During cell culture, the cells from (B) border areas (1 mm long), (NB) near border areas (1 mm long, 5 mm to the near border) and (C) central areas (1 mm long) as pointed by black arrows were monitored continuously.

(b) Schematic diagram of the cross sections of the horizontal SDCM with 8 short connected capillaries. (1) Short capillaries (Length: 10 mm) were joined together using (2) oxygen permeable short silicone tubes (3mm long) and horizontally suspended using 2 pieces of (3) square silicone chips (4 mm × 4 mm, 0.5 mm thick). The connected capillary was then situated in a (4) plastic petri-dish. After system sterilization, (5) cell suspension (2×10^5 cells ml^{-1}) was added and incubated for 2 hours, and (6) media were added into the petri-dish for cell culture. During cell culture, the cells from (B) border areas (1 mm long), (NB) near border areas (1 mm long, 5 mm to the near border) and (C) central areas (1 mm long) as pointed by black arrows were monitored continuously.

(c) Schematic diagram of the cross sections of the vertical SDCM. (1) Short capillaries (Length: 10 mm) were vertically inserted into the small holes created in a (2) horizontally orientated silicone sheet with three (3) short glass rods attached underneath as the legs. After system sterilization, the supporting silicone sheet was rotated to keep the short capillaries horizontal, (4) cell suspension (2×10^5 cells ml^{-1}) was added into the lower end of the capillary and incubated for 1-2 hours for cell attachment, the short capillaries were then re-orientated vertically and situated in a (5) plastic petri-dish, and (6) fresh media were added into the dish to submerge the lower part of the capillary with seeded cells for cell culture. During cell culture, the cells at the lower end of the capillary (1 mm long) as pointed by the black arrow were monitored continuously.

Live cell fluorescent and confocal microscopy using Cell Tracker™

The live-cell staining protocol for monolayer cell culture was adopted with slight modifications. Briefly, the media inside the capillaries were gently removed and replaced by the same amount of fresh media with 10 μM fluorescent probe Cell Tracker™ Red CMTPX (C34552, Invitrogen). After incubated for 24 hours at 37°C and 5% CO_2, the Cell Tracker™ reagent was replenished with fresh media. Cell culture was then continued and the fluorescently labeled cells were analyzed using fluorescent (Nikon Ti, Japan) or confocal microscopes (Nikon Cl, Japan) at λ_{ex}= 580nm, λ_{em}= 650 nm (for TRITC / Cell Tracker™ visualization). After culture, the cells were fixed in 4% (w/v) paraformaldehyde in PBS for further microscopic analysis.

Immuno-fluorescent microscopy

The conventional immune-staining protocol with Phalloidin-FITC for monolayer cell culture was also modified for the SDCMs.

Briefly, the media in each of the capillaries were gently removed after cell culture. The cells inside were washed with PBS (×3), fixed in 4% (w/v) paraformaldehyde for 30 min, and permeabilised with 0.2% (w/v) Triton X-100 in PBS for 30 min, washed gently with PBS (×3) for 24 hours. After incubated with Phalloidin-FITC (Sigma, 20 μM) for 24 hours, washed gently with PBS (×3) for another 24 hours, fluorescent micrographs of the immune-stained individual or aggregated cells were captured using a fluorescent microscope (Nikon Ti, Japan) or a confocal microscope (Nikon Cl, Japan) at λ_{ex}= 495 nm, λ_{em}= 515 nm (for Phalloidin-FITC / F actin visualization).

Viability assessment using MTT assay

Viable cells inside the capillaries were also assessed using MTT assay. Briefly, the cultured cells inside the capillaries were washed gently with PBS and then incubated in MTT solution (0.5 mg ml^{-1} in PBS) for 2 hours at 37°C. Subsequently, the solution was aspirated and the insoluble formazan product was solubilized with DMSO for 10 min, and the optical density at 550 nm was measured using a plate reading spectrophotometer.

Statistics

Student's unpaired *t*-test was used to compare cell viabilities under different culture conditions (*p<0.05, **p<0.01, ***p<0.001).

Results

Continuous and noninvasive *in situ* cell assessment during tissue culture

Capillaries with fixed ID (1.0 mm) and varying lengths (10, 30, 60, 80 mm) were used to mimic the interconnected pore structures in porous scaffolds. Preliminary experiments using the longest capillaries (80 mm) indicated that the optimal culture time period for maximum live cells was approximately 20 days. Thus in this experiment, HDFs at different parts of these vessels were assessed noninvasively for 20 days. Phase-contrast microscopic analysis indicated that at earlier culture stages (1-2 days), HDFs spread, migrated and orientated randomly on the inner surfaces of all the capillaries as shown in Figure 2a-i. As culture progressed, only the cells at border and near border areas (within the range of approximately 5-10 mm) maintained normal morphologies and aligned with each other (Figure 2a-ii), while very few cells or cell debris were observed in the central areas (Figure 2b-iii). After cultured for 7-12 days, some HDFs within the border areas were observed to detach, aggregate and coordinate to bridge the inner surfaces of the capillaries. As more cells joined in, large cell aggregates with complex 3D structures were formed as shown in Figure 2b-i.

After cultured for 20 days, the cells were immune-stained for confocal fluorescent microscopy. Aggregated cells were imaged only within border areas as show in Figures 3a and 3b. Further optical sectioning analysis indicated that the 3D cell aggregates were closely linked with the cell monolayers on the inner surfaces of the capillaries through elongated or stretched cells; and the overall morphologies of the cell clusters were extremely irregular as shown in Figure 3c. HDFs were also cultured in vertical capillaries (ID: 1.0 and 1.5 mm, Length: 10 mm) for 20 days, live stained and assessed from a different perspective using confocal fluorescent microscope; and very similar results were obtained as illustrated in Figure 3d.

Viability assay of the cells cultured in horizontal systems

HDFs were cultured in capillaries with fixed ID (1.0 mm) and varying lengths (10, 30, 60, 80 mm) for 20 days, and then analyzed using MTT assay. As Figures 4a and 4b illustrated, the averaged cell

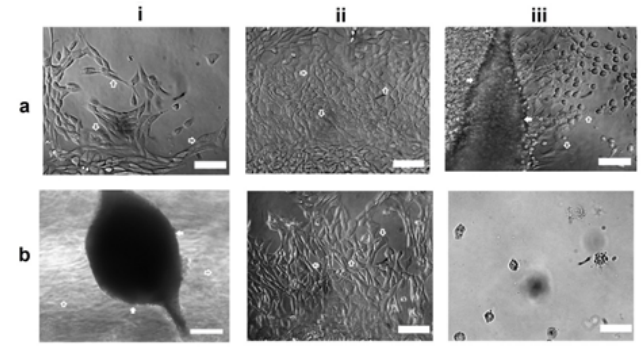

Figure 2: Phase contrast micrographs of human dermal fibroblasts (HDFs) cultured in glass capillaries (Length: 80 mm, ID=1.0 mm). **(a)** HDFs (2×10^5 cells ml^{-1}) seeded in the capillaries were cultured continuously and imaged noninvasively. The micrographs shown were captured at (i) 1, (ii) 4 and (iii) 12 days in the (B) border areas. **(b)** Micrographs of HDFs from (B) border areas (i), (NB) near border areas (ii) and (C) central areas (iii) of the capillaries were captured after cultured for 20 days. Cell monolayers and aggregates are indicated by open and closed arrows respectively. Scale bar=100 μm.

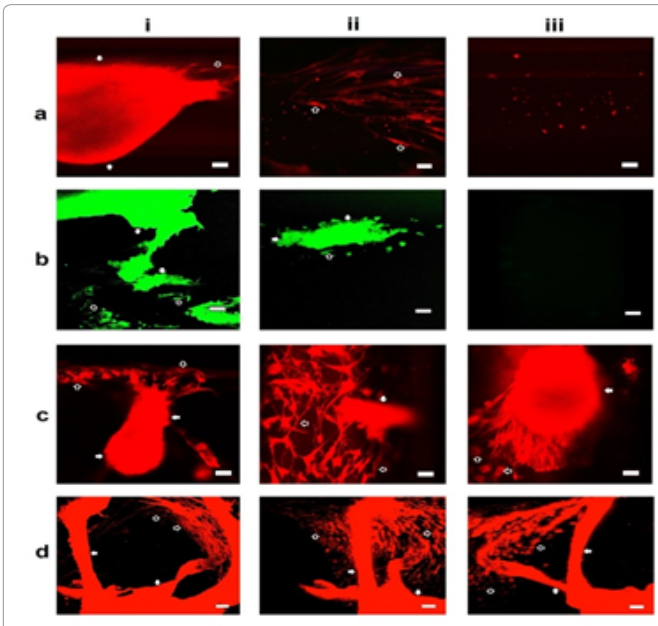

Figure 3: Confocal fluorescent micrographs of human dermal fibroblasts (HDFs) cultured in the horizontal and vertical SDCMs. HDFs (2 × 10^5 cells ml^{-1}) seeded in horizontal capillaries (Length: 80 mm, ID=1.0 mm) were cultured for 20 days and stained using **(a)** Cell Tracker™ (Red), **(b)** Phalloidin-FITC (Green). Micrographs shown were captured from (B) border areas (i), (NB) near border areas (ii) and (C) central areas (iii). HDFs (2 × 10^5 cells ml^{-1}) seeded in **(c)** horizontal capillaries (Length: 80 mm, ID= 1.0 mm) and **(d)** vertical capillaries (Length: 10 mm, ID: 1.5 mm) were cultured for 20 days, stained using Cell Tracker™ (Red). The micrographs of different cell aggregates shown in (i-iii) were captured using optical sectioning. Cell monolayers and cell aggregates are indicated by open and closed arrows respectively. Scale bar=100 μm.

viabilities across short capillaries (10 mm) were significant higher than those across longer capillaries (30-80 mm). Further experiments indicated that the culture period for optimal cell viability in capillaries with fixed ID (1.0 mm) and length (80 mm) was approximately 20 days (Figure 4c), which confirmed our preliminary experiments. In order to understand the influence of oxygen permeability of the vessel material on cell viability, capillaries with different lengths (30, 60, 80 mm) were fabricated by connecting short capillaries (ID: 1.0 mm, length: 10 mm)

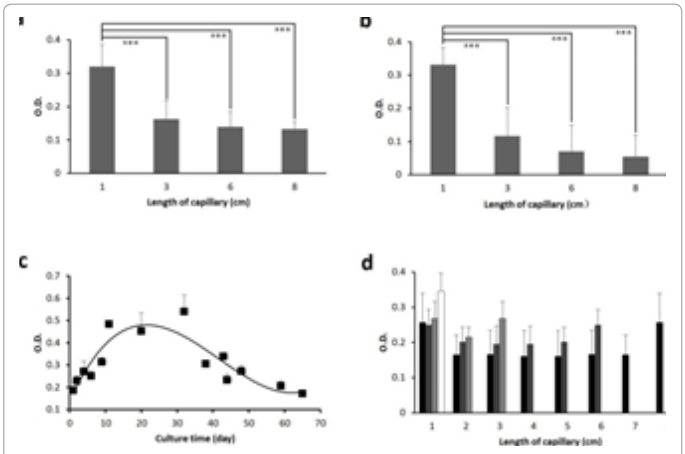

Figure 4: MTT viability assay of human dermal fibroblasts (HDFs) cultured in the horizontal SDCMs. HDFs (2 × 10^5 cells ml^{-1}) seeded in the capillaries with varying lengths (10, 30, 60, 80 mm) and defined inside diameter (1.0 mm), cultured for 20 days, stained with MTT, **(a)** varying volumes of DMSO (200, 600, 1200, 1600 µl) were used to dissolve formazan from capillaries with varying lengths (10, 30, 60, 80 mm) for MTT assay; **(b)** defined volumes of DMSO (200 µl) were used to dissolve formazan in each capillary, but the O.D. values averaged to 10mm of the capillaries were plotted. **(c)** HDFs (2×10^5 cells ml^{-1}) seeded in the capillaries (Length: 80 mm, ID: 1.0 mm) and culture for cultured for different time periods (from 1 to 65 days), and assessed using MTT. **(d)** HDFs (2×10^5 cells ml^{-1}) seeded and cultured in connected capillaries with varying lengths (White: 10 mm, Light grey: 30 mm, Dark grey: 60 mm, Black: 80 mm) and defined inside diameter (1.0 mm). After cultured for 20 days, all the short capillaries (10 mm) were disconnected and the cells inside were assessed using MTT. Results shown are means ± standard deviation of triplicate experiments.

with silicone tubes (oxygen permeability coefficient at 25°C: 600 Barrer, approximately 400 times higher than that butyl rubber, and 60 times higher than that of polystyrene), and used to culture HDFs for 20 days. The short glass capillaries were then disconnected and analyzed separately using MTT assay. As shown in Figure 4d, viable cells were detected across all the connected capillaries, which was confirmed by microscopic analysis (images not shown).

The influences of interconnected pore sizes on cell survival

To investigate the influences of interconnected open pores within thick scaffolds on the infiltrated cells, HDFs were seeded in capillaries with defined length (80 mm) and varying IDs (0.3, 1.0, 1.7, 2.2 mm) and cultured for 20 days for confocal fluorescent microscopy. The IDs demonstrated obvious influences on cell survival as cells were detected in more areas deep inside the capillaries as the ID increased from 1.0 to 2.2 mm (Figure 5). Cells with normal spindle morphologies were even observed in the central areas of the thick capillaries (ID: 2.2 mm) as shown in Figure 5d-iii, while almost no cell was detected in the central areas of thin capillaries (ID: 0.3 mm) as illustrated in Figure 5a-iii.

The influences of media replenishment on cell survival

HDFs seeded in capillaries (ID: 1.0 and 1.5 mm, Length: 80 mm) were divided into 3 groups. The media inside the capillaries for the first and second groups were deliberately replenished with fresh media every day (CED) and twice a week (CTW) respectively, while in the third group the media inside the capillaries were not replenished (NC) during the whole culture time period. For all these 3 groups, the media in the petri-dishes were replenished twice a week. After cultured for 20 days, the cells inside all the capillaries were immune-stained for confocal fluorescent microscopy. As shown in Figure 6, cells with normal morphologies were detected across the capillaries in CED/

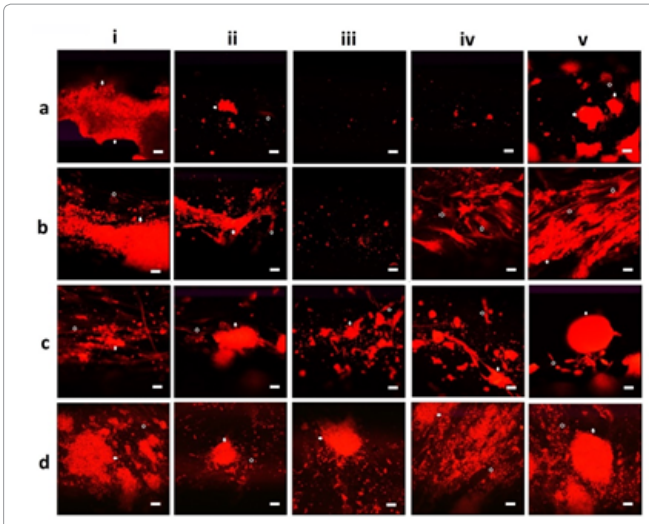

Figure 5: Confocal fluorescent micrographs of human dermal fibroblasts (HDFs) cultured in glass capillaries with fixed length (80 mm) and varying inside diameters. HDFs (2 × 105 cells ml-1) seeded in the capillaries with varying inside diameters of (a) 0.3 mm; (b) 1.0 mm; (c) 1.7 mm; and (d) 2.2 mm; cultured for 20 days, stained using Cell TrackerTM (Red). Micrographs shown were captured at border areas (i, v), near border areas (ii, iv) and central areas (iii). Cell monolayers and cell aggregates are indicated by open and closed arrows respectively. Scale bar=100 µm.

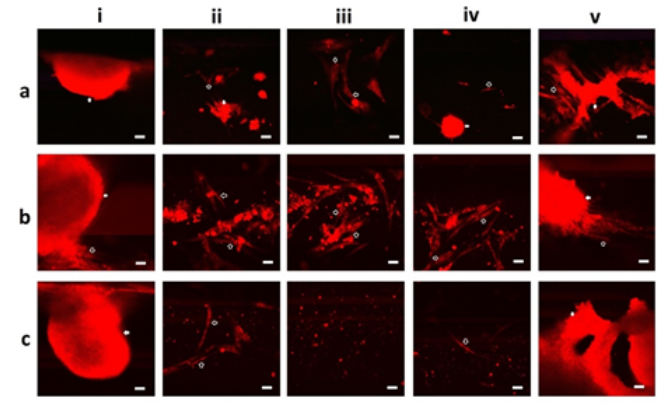

Figure 6: The influences of medium replenishment on the survival of human dermal fibroblasts (HDFs) cultured in capillaries (Length: 80 mm, ID: 1.5 mm). HDFs (2 × 105 cells ml-1) seeded in the capillaries were cultured for 20 days. During culture the media inside the capillaries were replenished (a) everyday (CED), (b) twice a week (CTW), and in (c) the medium was not deliberately changed. After culture, the cells were stained using Cell TrackerTM. Micrographs shown were captured at border areas (i, v), near border areas (ii, iv) and central areas (iii). Cell monolayers and cell aggregates are indicated by open and closed arrows respectively. Scale bar=100 µm.

CTW groups, but no 3D cell clusters were detected in the central areas of these capillaries. In the NC group, both individual and aggregated cells were only observed within the border areas of the capillaries as expected.

Discussion

In Tissue Engineering, a variety of scaffolds have been designed and fabricated [19,20] as they play crucial roles by providing not only physical support but also biochemical and biomechanical stimulation to the cultivated cells [16,21]. Moreover, the overarching factors induced within large 3D porous scaffolds also have great impacts on

various cell behaviours [17,22,23]. Our mechanistic understanding of these regulatory factors within 3D scaffolds is still very limited [2,5,13], as tracking the dynamic tissue formation processes using conventional tissue culture systems is often technically infeasible [24,25]. It is especially problematic to achieve rapid and reliable *in situ* measurements of the infiltrated cells in thick scaffolds without sacrificing the samples [26]. Although very thin scaffold membranes or films have been employed for the ease of continuous *in situ* cell analysis [13,22,27], they are usually too thin to represent the anisotropic properties of the thick scaffolds [28], thus the aim of this research was to design and fabricate a set of SDCMs to mechanistic understanding of the infiltrated in thick porous scaffolds. Since the infiltrated cells within the SDCMs were not sacrificed by conventional sectioning processes, it was possible to analyse the delicate 3D cell structures using different optical microscopic technologies, which is crucially important for the understanding of tissue formation at cellular levels. Apart from microscopic analysis, cell viabilities within the SDCMs were also assessed using conventional MTT assay with slight modifications. Our evaluation experiments indicated that these SDCMs were able to mimic complex culture environments within large porous scaffolds such as the nutrient/waste gradients that demonstrated significant influences on the survival of the cultivated cells. Media replenishment experiments confirmed that the cell necrosis deep inside the long capillaries was mainly due to the limited mass transfer. Further investigations using capillaries connected by oxygen permeable silicone tubes suggested that oxygen diffusion was one of the limiting factors for cell survival in large porous scaffolds. The significant impacts of open pore structures on cultivated cells were recognized but still poorly understood [22,23,29]. Our cell culture experiments using capillaries with different inside diameters provided crucial clues about the influences of open pores on 3D tissue formation. HDFs usually grow in monolayer on flat surfaces such as tissue culture plates, but they formed complex 3D cell aggregates within the capillary vessels. Optical sectioning using confocal fluorescent microscope demonstrated that these 3D cell clusters were closely linked with the cell monolayer on the inner capillary surfaces through elongated single and bundled cells, suggesting the contribution of both curved surfaces and cell monolayers on cell aggregations. Compared to monolayer of cells on tissue culture surfaces, the cells that formed the 3D cell structures were observed to be tightly packed as previously described [30], and the overall appearances of the cell aggregates were extremely irregular. Our simple medium replenishment experiments suggested that media perfusion might be another element that influenced cell aggregations, as almost no obvious 3D cell structures were observed in the central areas of the capillaries for medium replenishment. For further understanding, more detailed investigations of the influences of media perfusion with defined flow rates on tissue formation are necessary. In this research, other parameters such as scaffold thickness, open pore size and culture time period on optimal cell survival were also investigated using both *in situ* microscopy and MTT assay.

The SDCMs designed in this research demonstrated various advantages. First of all, they are suitable for parallelized cell cultures. Compared with similar studies using porous scaffolds [31,32], these systems enable experimentalists to quickly set-up multiple parallel cultures to mimic various 3D micro-environments within scaffolds of different thicknesses and open pore structures, which can be used to systematically distinguish and investigate the influences of different regulatory factors or biological processes on the formation of engineered tissues. Secondly, rapid and reliable *in situ* assessment of infiltrated cells. Due to the use of transparent and low auto-fluorescent glass capillaries as the culturing vessels, *in situ* imaging with high resolution and morphological characterization of live cells infiltrated deep inside the long capillaries can be conducted non-invasively for days, weeks and even months simply using conventional microscopic technologies. Thirdly, ease to use. As all the cell culture capillaries were situated in normal plastic petri-dishes, various experimental operations such as system sterilization, cell seeding, culturing, immune-staining and *in situ* microscopic assessments can be carried out consecutively. Finally, low cost. All the components such as medical glass capillaries, silicone gaskets and plastic petri-dishes are commonly used consumables and commercially available, thus these cell culture systems can be established in any tissue or cell culture laboratories with very low cost.

Due to the aforementioned advantages, these SDCMs can be employed for very different purposes. For example, by coating the inner surfaces of the glass capillary vessels with various biomaterials, they can be used to screen putative cellular microenvironments by testing different ECM components and other synthetic or natural materials; which will facilitate the design and fabrication of more functional scaffolds. As the presence of monolayer and 3D cell structures is crucial for efficient drug screening [33], and both were observed in the capillary vessels, these SDCMs will be also evaluated for its potential for high through-put screening of drugs.

Conclusion

A set of SDCMs have been designed to provide the needed resolution, standardization and culture environments analogous to the conditions surrounding the infiltrated cells within large scaffolds. As both individual and aggregated cells within these *in vitro* models can be imaged noninvasively and continuously using conventional microscopic technologies, it is feasible to track the dynamic tissue development processes for mechanistic understanding. Due to the coexistence of cell monolayer and cell aggregates, these SDCMs can also be evaluated for high through-put screening of drugs.

Acknowledgment

This work was supported by the RDF (Research Development Fund) from XJTLU. We would like to acknowledge the colleagues in the Centre of Biological Engineering at Loughborough University for their comments and suggestions of this manuscript.

References

1. Zonari A, Novikoff S, Electo NRP, Breyner NM, Gomes DA, et al. (2012) Endothelial differentiation of human stem cells seeded onto electrospun polyhydroxybutyrate/polyhydroxybutyrate-co-hydroxyvalerate fiber mesh. PLoS ONE 7: e35422.
2. Gurtner GC, Chapman MA (2016) Regenerative medicine: Charting a new course in wound healing. Adv Wound Care 5: 314–328.
3. Baiguera S, Urbani L, Del Gaudio C (2014) Tissue engineered scaffolds for an effective healing and regeneration: Reviewing orthotopic studies. Biomed Res Int 2014: e398069.
4. Scarritt ME, Pashos NC, Bunnell B (2015) A review of cellularization strategies for tissue engineering of whole organs. Front Bioeng Biotechnol 3: 43.
5. de Kemp V, de Graaf P, Fledderus JO, Ruud Bosch JLH, de Kort LMO (2015) Tissue engineering for human urethral reconstruction: Systematic review of recent literature. PLoS ONE 10: e0118653.
6. de la Puente P, Muz B, Gilson RC, Azab F, Luderer M, et al. (2015) 3D tissue-engineered bone marrow as a novel model to study pathophysiology and drug resistance in multiple myeloma. Biomaterials 73: 70-84.
7. Knight E, Przyborski S (2015) Advances in 3D cell culture technologies enabling tissue-like structures to be created in vitro. J Anat 227: 746-756.
8. Rogozhnikov D, O'Brien PJ, Elahipanah S, Yousaf MN (2016) Scaffold free bio-orthogonal assembly of 3-Dimensional cardiac tissue via cell surface

engineering. Sci Rep 6:39806.

9. Wrzesinski K, Fey SJ (2015) From 2D to 3D--a new dimension for modelling the effect of natural products on human tissue. Curr Pharm Des 21: 5605-5616.
10. Lin H, Godiwalla SY, Palmer B, Frimberger D, Yang Q, et al. (2014) Understanding roles of porcine small intestinal submucosa in urinary bladder regeneration: Identification of variable regenerative characteristics of small intestinal submucosa. Tissue Eng Part B Rev 20: 73-83.
11. Yang C, Deng G, Chen W, Ye X, Mo X (2014) A novel electrospun-aligned nanoyarn-reinforced nanofibrous scaffold for tendon tissue engineering. Colloids Surf B Biointerfaces 122: 270–276.
12. Lowenthal J, Gerecht S (2016) Stem cell-derived vasculature: A potent and multidimensional technology for basic research, disease modeling, and tissue engineering. Biochem Biophys Res Commun 473: 733–742.
13. Gabbott CM, Zhou ZX, Han GX, Sun T (2017) A novel scale-down cell culture and imaging design for the mechanistic insight of cell colonisation within porous substrate. J Microsc 267: 150-159.
14. Boxberger HJ, Meyer TF (1994) A new method for the 3-D in-vitro growth of human Rt112 bladder-carcinoma cells using the alginate culture technique. Biol Cell 82: 109-119.
15. Berthiaume F, Maguire JT, Yarmush ML (2011) Tissue engineering and regenerative medicine: History, progress, and challenges. Annu Rev Chem Biomol Eng 2:403–430.
16. Mochizuki H, Ohnuki Y, Kurosawa H (2011) Effect of glucose concentration during embryoid body (EB) formation from mouse embryonic stem cells on EB growth and cell differentiation. J Biosci Bioeng 111: 92-97.
17. Rustad KC, Sorkin M, Levi B, Longaker MT, Gurtner GC (2010) Strategies for organ level tissue engineering. Organogenesis 6: 151-157.
18. Sun T, Haycock J, MacNeil S (2006) In situ image analysis of interactions between normal human keratinocytes and fibroblasts cultured in three-dimensional fibrin gels. Biomaterials 27: 3459–3465.
19. Grayson WL, Martens TP, Eng GM, Radisic M, Vunjak-Novakovic G (2009) Biomimetic approach to tissue engineering. Semin Cell Dev Biol 20: 665-673.
20. Meng X, Leslie P, Zhang Y, Dong J (2014) Stem cells in a three-dimensional scaffold environment. Springerplus 3: 80.
21. Lesman A, Notbohm J, Tirrell AD, Ravichandran G (2014) Contractile forces regulate cell division in three-dimensional environments. J Cell Biol 205: 155-162.
22. Sun T, Donoghue PS, Higginson JR, Gadegaard N, Barnett SC, et al. (2011) The interactions of astrocytes and fibroblasts with defined pore structures in static and perfusion cultures. Biomaterials 32: 2021-2031.
23. Szentivanyi A, Chakradeo T, Zernetsch H, Glasmacher B (2011) Electrospun cellular microenvironments: Understanding controlled release and scaffold structure. Adv Drug Deliv Rev 63: 209-220.
24. Cosgrove DB, Griffith GL, Lauffenburger AD (2008) Fusing tissue engineering and systems biology toward fulfilling their promise. Cell Mol Bioeng 1: 33-41.
25. O'Dea RD, Byrne HM, Waters SL (2012) Continuum modelling of in vitro tissue engineering: A review. Stud Mechanobiol Tissue Eng Biomater 10: 229–266.
26. Baradez MO, Marshall D (2011) The use of multidimensional image-based analysis to accurately monitor cell growth in 3D bioreactor culture. PLoS One 6:e26104.
27. Hong JK, Madihally SV (2011) Next generation of electrosprayed fibers for tissue regeneration. Tissue Eng Part B Rev 17: 125-142.
28. Phipps MC, Clem WC, Grunda JM, Clines GA, Bellis SL (2012) Increasing the pore sizes of bone-mimetic electrospun scaffolds comprised of polycaprolactone, collagen I and hydroxyapatite to enhance cell infiltration. Biomaterials 33: 524-534.
29. Rnjak-Kovacina J, Weiss AS (2011) Increasing the pore size of electrospun scaffolds. Tissue Eng Part B Rev 17: 365-372.
30. Engelmayr GC, Papworth GD, Watkins SC, Mayer JE, Sacks MS (2006) Guidance of engineered tissue collagen orientation by large-scale scaffold microstructures. J Biomech 39: 1819–1831.
31. Ma T, Li Y, Yang ST, Kniss DA (2000) Effects of pore size in 3-D fibrous matrix on human trophoblast tissue development. Biotechnol Bioeng 70: 606-618.
32. Sundararaghavan HG, Burdick JA (2011) Gradients with depth in electrospun fibrous scaffolds for directed cell behavior. Biomacromolecules 12: 2344-2350.
33. Pontes-Soares C, Midlej V, de Oliveira ME, Benchimol M, Costa ML, et al. (2012) 2D and 3D-organized cardiac cells shows differences in cellular morphology, adhesion junctions, presence of myofibrils and protein expression. PLoS ONE 7: e38147.

Citation: Yu L, Cai MSc, Han G, Sun T (2017) Mechanistic Insights of the Infiltrated Cells in Large Porous Scaffolds Based on Microscopic Analysis of the Cells in Novel Scale-Down Culture Systems. Int J Microsc 1: 101.